



HAL
open science

Tetranuclear [Fe II 2 Fe III 2] 2+ molecular switches [Fe II (bik) 2 (N-) 2]spin-crossover complexes containing [Fe III (Tp)(CN) 3] – metalloligands as N-donor

D. Garnier, A. Mondal, Y. Li, P. Herson, L.-M. Chamoreau, Loic Toupet, Marylise Buron-Le Cointe, E.M.B. Moos, F. Breher, R. Lescouezec

► **To cite this version:**

D. Garnier, A. Mondal, Y. Li, P. Herson, L.-M. Chamoreau, et al.. Tetranuclear [Fe II 2 Fe III 2] 2+ molecular switches [Fe II (bik) 2 (N-) 2]spin-crossover complexes containing [Fe III (Tp)(CN) 3] – metalloligands as N-donor. Comptes Rendus. Chimie, 2019, 22 (6-7), pp.516-524. 10.1016/j.crci.2019.04.003 . hal-02161137

HAL Id: hal-02161137

<https://hal-univ-rennes1.archives-ouvertes.fr/hal-02161137>

Submitted on 20 Jul 2022

HAL is a multi-disciplinary open access archive for the deposit and dissemination of scientific research documents, whether they are published or not. The documents may come from teaching and research institutions in France or abroad, or from public or private research centers.

L'archive ouverte pluridisciplinaire **HAL**, est destinée au dépôt et à la diffusion de documents scientifiques de niveau recherche, publiés ou non, émanant des établissements d'enseignement et de recherche français ou étrangers, des laboratoires publics ou privés.



Distributed under a Creative Commons Attribution-NonCommercial 4.0 International License

Tetranuclear $[\text{Fe}^{\text{II}}_2\text{Fe}^{\text{III}}_2]^{2+}$ molecular switches: $[\text{Fe}^{\text{II}}(\text{bik})_2(\text{N-})_2]$ spin-crossover complexes containing $[\text{Fe}^{\text{III}}(\text{Tp})(\text{CN})_3]^-$ metalloligands as N-donor [#]

[#]This work is dedicated to Professor Michel Verdaguer

Delphine Garnier,^{a,b} Abhishake Mondal,^a Yanling Li,^a Patrick Herson,^a Lise-Marie Chamoreau,^a Loic Toupet,^c Marylise Buron Le Cointe,^c E.M.B. Moos,^b Frank Breher,^b Rodrigue Lescouëzec^a

Keywords: photomagnetism, spin-crossover complex, Fe^{II} , cyanide ligand

^a Institut Parisien de Chimie Moléculaire - CNRS UMR 8232, Sorbonne Université, 4 place Jussieu, F-75252 Paris cedex 05 France.

^b Institute of Inorganic Chemistry, Karlsruhe Institute of Technology (KIT), Engesserstr. 15, Geb. 30.45, D-76131 Karlsruhe, Germany.

^c Univ Rennes, CNRS, IPR (Institut de Physique de Rennes) - UMR 6251, F-35000 Rennes, France.

Abstract: Three novel mixed valence cyanide-bridged $\{\text{Fe}^{\text{III}}_2\text{Fe}^{\text{II}}_2\}$ square complexes were obtained through the self-assembling of $[\text{Fe}^{\text{III}}(\text{Tp})(\text{CN})_3]^-$ or $[\text{Fe}^{\text{III}}(\text{Tp}^*)(\text{CN})_3]^-$ cyanido building blocks with the in-situ formed $[\text{Fe}^{\text{II}}(\text{bik})_2(\text{S})_2]$ complex (Tp = hydrotris(pyrazol-1-yl)borate, Tp^* = hydrotris(3,5-dimethyl-pyrazol-1-yl)borate, bik = bis(1-methylimidazol-2-yl)ketone, **S = solvent**). The structure of these three complexes (**2**, **3** and **4**) are reminiscent of that of our previously published square complex $\{[\text{Fe}^{\text{III}}(\text{Tp})(\text{CN})_3]_2[\text{Fe}^{\text{II}}(\text{bik})_2]_2\} \cdot [\text{Fe}^{\text{III}}(\text{Tp})(\text{CN})_3]_2 \cdot 18\text{H}_2\text{O} \cdot 4\text{CH}_3\text{OH}$ (**1**). They consist of cyanide-bridged square dicationic complexes, ClO_4^- (**2** and **3**) or BF_4^- (**4**) counter ions and solvate molecules. The FT-IR cyanide stretching vibrations observed at $\nu_{\text{CN}} \approx 2145\text{-}60\text{ cm}^{-1}$ are typical of $\{\text{Fe}^{\text{III}}\text{-CN-Fe}^{\text{II}}\}$ moieties. The investigation of the magnetic properties of **2** reveals the occurrence of spin-crossover centred at $T_{1/2} = 227\text{ K}$. The $\chi_M T$ variation, *ca.* $7\text{ cm}^3\text{ mol}^{-1}\text{ K}$, reflects the complete spin-state change occurring on both $\{\text{Fe}^{\text{II}}(\text{bik})(\text{-NC})_2\}$ moieties (-NC represent the cyanido building blocks). The Slichter-Drickammer model leads to a weak cooperativity factor, $\Gamma = 1.6\text{ kJ.mol}^{-1}$ (with $\Gamma \ll \text{kJ.mol}^{-1}$), which reflects the gradual spin-state change. This is in agreement with the molecular structure of **2**, which does not present significant intermolecular interactions. The calculated enthalpy and entropy variation associated to the spin-state equilibrium are $\Delta H = 24\text{ kJ.mol}^{-1}$ and $\Delta S = 105\text{ J.K}^{-1}\text{.mol}^{-1}$. In contrast **3** and **4** show only partial spin crossover in the accessible temperature range (2 - 400 K) as the $T_{1/2}$ are shifted toward higher temperatures (*ca.* $T_{1/2} > 400\text{ K}$). While no photomagnetic effect is observed for **3**, compound **4** shows a moderate increase of the magnetization upon irradiation at low temperature. This phenomenon is ascribed to the Light-Induced Excited Spin-State Trapping (LIESST) effect. Interestingly, the complex **2** also

shows a remarkable LIESST effect, which is observed with different laser lights covering the visible and NIR range. The resulting $\chi_M T$ value obtained in the photoinduced state suggests the occurrence of a ferromagnetic interaction inside the $\{\text{Fe}^{\text{III}}\text{-CN-Fe}^{\text{II}}\}$ units.

Mots clés: photomagnétisme, complexe à transition de spin, Fe^{II} , ligand cyanure

Résumé: Trois nouveaux complexes carrés $\{\text{Fe}^{\text{III}}_2\text{Fe}^{\text{II}}_2\}$ à pont cyanure et à valence mixte ont été obtenus par auto-assemblage des précurseurs cyanurés $[\text{Fe}^{\text{III}}(\text{Tp})(\text{CN})_3]^-$ ou $[\text{Fe}^{\text{III}}(\text{Tp}^*)(\text{CN})_3]^-$ et du complexe cationique $[\text{Fe}^{\text{II}}(\text{bik})_2(\text{S})_2]$ formé in-situ (Tp = hydrotris(pyrazol-1-yl)borate, Tp^* = hydrotris(3,5-diméthyl-pyrazol-1-yl)borate, bik = bis(1-méthylimidazol-2-yl)cétone, **S = solvant**). Les structures de ces trois complexes (**2**, **3** et **4**) sont similaires à celle du complexe $\{[\text{Fe}^{\text{III}}(\text{Tp})(\text{CN})_3]_2[\text{Fe}^{\text{II}}(\text{bik})_2]_2\} \cdot [\text{Fe}^{\text{III}}(\text{Tp})(\text{CN})_3]_2 \cdot 18\text{H}_2\text{O} \cdot 4\text{CH}_3\text{OH}$ (**1**) préalablement publié. Elles sont constituées de complexes carrés dicationiques à pont cyanure, de contre-ions ClO_4^- (**2** and **3**) ou BF_4^- (**4**) et de molécules de solvant. Les vibrations d'élongation des cyanures, observée en spectroscopie IR à $\nu_{\square\square} \approx 2145\text{-}60\text{ cm}^{-1}$, sont caractéristiques d'unités $\{\text{Fe}^{\text{III}}\text{-CN-Fe}^{\text{II}}\}$. L'étude des propriétés magnétiques de **2** révèle un équilibre de spin centré à $T_{1/2} = 227\text{ K}$. La variation du produit $\chi_M T$, *ca.* $7\text{ cm}^3\text{ mol}^{-1}\text{ K}$, traduit une conversion de spin complète sur **chacune des unités** $\{\text{Fe}^{\text{II}}(\text{bik})(\text{-NC})_2\}$ du carré (-NC représente le complexe précurseur cyanuré). L'analyse des données par le modèle de Slichter-Drickammer conduit à un faible facteur de coopérativité, $\Gamma = 1.6\text{ kJ}\cdot\text{mol}^{-1}\text{ K}$ (with $\Gamma \square \square\square\square\square\square$), en accord avec un changement d'état de spin graduel. Ces données sont en accord avec la structure de **2** qui ne montre pas d'interactions intermoléculaires notables. **Les** valeurs des variations d'enthalpie et d'entropie associées à la conversion de spin sont $\Delta H = 24\text{ kJ}\cdot\text{mol}^{-1}$ et $\Delta S = 105\text{ J}\cdot\text{K}^{-1}\cdot\text{mol}^{-1}$. Au contraire de **2**, les composés **3** and **4** présentent seulement une conversion de spin partielle dans le domaine de température exploré (2 - 400 K) avec des valeurs $T_{1/2}$ déplacées vers les hautes températures (*ca.* $T_{1/2} > 400\text{ K}$). Tandis qu'on n'observe pas d'effet photomagnétique pour **3** et seulement un faible effet dans **4**, le composé **2** présente une forte augmentation de son aimantation sous irradiation à basse température. Cet effet est dû au piégeage photo-induit d'un état excité de spin (effet « LIESST », Light-Induced Excited Spin-State Trapping) Il est observé avec différentes sources laser couvrant le spectre visible et le proche IR. Les valeurs de $\chi_M T$ obtenues dans l'état photo-induit suggèrent la présence d'une interaction ferromagnétique au sein de la paire $\{\text{Fe}^{\text{III}}\text{-CN-Fe}^{\text{II}}\}$.

1 Introduction and background

Switchable molecular systems featuring electronic, magnetic, or optical bistability are attracting a strong research interest because of their potential use as molecular memories, switches, actuators, or sensors. [1–3] Although their integration into actual devices is challenging, various encouraging results show promise in emerging fields such as molecular electronics.[4–7] The cyanide coordination chemistry has proven successful in providing access to a variety of responsive systems, whose optical and magnetic properties can be reversibly switched.[8–10] One of the emblematic examples are the FeCo Prussian blue analogues, which show an increase of magnetization under light irradiation.[11] In these materials, the so-called photomagnetic effect was ascribed to a metal-metal electron transfer coupled to a spin-state change induced by light irradiation.[12,13] The system can then relax from the photo-induced metastable state to the ground state upon heating. Since few years various groups have been investigating polymetallic complexes showing photomagnetism.[14,15] In order to reduce the dimensionality of the FeCo PBAs, a common strategy is based on the use of $[\text{Fe}^{\text{III}}(\text{L})(\text{CN})_x]^-$ metalloligand toward partially blocked Co precursors.[16] More specifically, many of these systems were obtained with *fac*- $[\text{Fe}^{\text{III}}(\text{Tp})(\text{CN})_3]^-$ building blocks, where the Tp is a derivative of the hydrotris(pyrazol-1-yl)borate scorpionate ligand. These low dimensional systems can be used as model to better understand the photomagnetic properties[17,18] or they can also be integrated using soft chemistry approaches into molecule based devices[19]. In the last years we have been interested in the study of $\{\text{Fe}_2\text{Co}_2\}$ squares obtained by self-assembling the $[\text{Fe}^{\text{III}}(\text{Tp})(\text{CN})_3]^-$ with partially blocked $[\text{Co}(\text{bik})_2(\text{S})_2]$ complexes (S = solvent, bik = bis(1-methylimidazol-2-yl)ketone).[16,20,21] Additionally, we also explored the use of $[\text{Fe}^{\text{III}}(\text{Tp})(\text{CN})_3]^-$ complexes as ligand toward other metal ions. The use of partially blocked Fe(II) complexes is of particular interest as the resulting material exhibits $\text{Fe}^{\text{II}}\text{N}_6$ coordination sites, which provide a suitable surrounding for observing spin-crossover phenomenon. As for the FeCo switchable materials, the spin-state change from the Fe^{II} low spin (LS) to the Fe^{II} high spin (HS) can be thermally induced and photo-induced at low temperature. In that case the photomagnetic properties arise from the so-called “Light-Induced Excited Spin State Trapping” (LIESST) effect. We first reported in 2012 the tetrametallic mixed-valence complex, $\{[\text{Fe}^{\text{III}}(\text{Tp})(\text{CN})_3]_2[\text{Fe}^{\text{II}}(\text{bik})_2]_2\} \cdot [\text{Fe}^{\text{III}}(\text{Tp})(\text{CN})_3]_2 \cdot 18\text{H}_2\text{O} \cdot 4\text{CH}_3\text{OH}$ (**1**), which exhibits a square core structure $\{\text{Fe}^{\text{III}}_2\text{Fe}^{\text{II}}_2\}$, while two $[\text{Fe}^{\text{III}}(\text{Tp})(\text{CN})_3]^-$ act as counter ions.[22] The spin-state changes occurring in this complex are very dependent on the solvation state of the material. The solvated phase shows a transition temperature located slightly above room temperature, $T_{1/2} = 330$ K, while in the desolvated phase the transition is shifted toward low temperatures, with $T_{1/2} = 240$ K. Moreover, the fresh solvated compound is not photomagnetic whereas the desolvated one shows an

efficient LIESST effect at 750 nm, with T_{relax} approx. 45 K (the relaxation temperature is measured by heating the sample at 0.3 K/min).

In the last years, we have decided to extend this work to study the influence of the N - donor on the switchable properties of the $[\text{Fe}^{\text{II}}(\text{bik})_2(N^-)_2]$ spin-crossover subunit, where N^- stands for N donor organic/inorganic ligand or metaloligands[23–25]. We observed that the spin transition temperature changed with the nature of the N^- donor (metallo)ligand. Different N^- donors can lead to different ligand field on the Fe(II) SCO units and thus a change in the LS / HS energy gap. However it is difficult to draw correlation in solid-state studies as other factors, such as the intermolecular interactions[26,27] or the inter-ligand interactions also affect the $T_{1/2}$. [28,29] For those cases where the compared spin-crossover complexes exhibit a similar structure such as in the case of the neutral $[\text{Fe}^{\text{II}}(\text{bik})_2(\text{NCX})_2]$ spin crossover complexes ($X= \text{S}, \text{Se}$) the rationalization of the properties is easier. Our experimental and theoretical study showed that the NCSe^- ligands induce a stronger ligand field than the NCS^- one, and thus a higher spin-crossover transition temperature, $T_{1/2}$. [24] Comparison between the transition temperatures of similar complexes are also easier to rationalize in solution studies, as the influence of the intermolecular interaction vanishes. For example, we have shown that it was possible to rationalize the transition temperature in the family $[\text{Fe}^{\text{R}}(\text{bik})_3]^{2+}$ and $[\text{Fe}(\text{bim})_3]^{2+}$ complexes (R are methyl, ethyl or vinyl groups grafted on the imidazolyl donors of the bik ligand; bim is similar to bik but the ketone is replaced by a methane group). Our experimental multitechnique approach led to results that are coherent with the theoretical prediction. Additionally, we showed in this study that among the different techniques used to follow the spin-crossover equilibrium (UV-vis, Evans NMR, magnetic measurements in solution), the monitoring of an adequately chosen ^1H NMR signal could be a very straightforward and accurate approach.

More interestingly, we have systematically studied all these $[\text{Fe}(\text{bik})_2(N^-)_2]$ systems by comparing the photomagnetic effect at 20 K by using different wavelengths in the visible and close infra-red regions (from 405 nm to 1313 nm). When replacing the $[\text{Fe}^{\text{III}}(\text{Tp})(\text{CN})_3]^-$ metalloligand with $[\text{Mo}^{\text{V}}(\text{CN})_8]^{3-}$, we obtained another square complex of formula $\{[\text{Mo}(\text{CN})_8]_2[\text{Fe}(\text{bik})_2]_2\}(\text{HMeIm})_2 \cdot 5\text{H}_2\text{O} \cdot \text{CH}_3\text{CN}$, which exhibits similar $[\text{Fe}^{\text{II}}(\text{bik})_2(N^-)_2]$ chromophores. [23] Here the thermally-induced spin transition is very gradual. It occurs near room temperature and it is accompanied by a solvent loss, that makes the spin-state change irreversible. The dehydrated compound is still photomagnetic with a close relaxation temperature (T_{relax} ca. 48 K). However the most efficient irradiation wavelength is located at 405 nm, which strikingly contrast with the situation observed in the previously reported $\{\text{Fe}^{\text{III}}_2\text{Fe}^{\text{II}}_2\}$ square, whose photomagnetic effect is higher near 750 nm. These results are to be compared with the model spin-crossover compound $[\text{Fe}^{\text{II}}(\text{bik})_3](\text{BF}_4)_2$, which shows a spin-crossover centered at $T_{1/2} = 316$ K and a photomagnetic effect, which is more efficient (but uncomplete) at 635 nm. Finally, in the

[Fe^{II}(bik)₂(NCX)₂] complexes, the photomagnetic effect is still observed although it is incomplete. The most efficient wavelength to promote a LIESST effect is 900 nm (while the induced magnetization is lower at 808 and 635 nm). However these system relax at 20 K (the temperature set of all our photomagnetic measurements) when switching off the light, indicating thus the existence of an efficient relaxation pathway. It is worth noticing that no significant difference are observed in the visible absorption spectra of the all these spin crossover compounds. They all exhibit a broad absorption centered at *ca.* 630 nm and ascribed to a Metal-Ligand Charge Transfer (MLCT). No MMCT are observed for the polymetallic square complexes. Continuing these experimental investigations, we looked here at the properties of three novel {Fe₂Fe₂}²⁺ square complexes

$$\{[\text{Fe}^{\text{III}}(\text{Tp}^*)(\text{CN})_3]_2[\text{Fe}^{\text{II}}(\text{bik})_2]\}_2(\text{ClO}_4)_2 \cdot 2\text{H}_2\text{O} \quad (2),$$

$$\{[\text{Fe}^{\text{III}}(\text{Tp})(\text{CN})_3]_2[\text{Fe}^{\text{II}}(\text{bik})_2]\}_2(\text{ClO}_4)_2 \cdot 2\text{CH}_3\text{CN} \quad (3),$$

$$\{[\text{Fe}^{\text{III}}(\text{Tp})(\text{CN})_3]_2[\text{Fe}^{\text{II}}(\text{bik})_2]\}_2(\text{BF}_4)_2 \cdot 2\text{CH}_3\text{OH} \quad (4)$$

(Tp = hydrotris(pyrazol-1-yl)borate, Tp* = hydrotris(3,5-dimethyl-pyrazol-1-yl)borate, bik = bis(1-methylimidazol-2-yl)ketone). On the one hand two different [Fe^{III}(L)(CN)₃]⁻ metalloligands were used, and on the other hand the counter ions are different so as the intermolecular interactions. Our purpose was to check in which extent the photomagnetic properties can be influenced by the metalloligand, the solid state structure and intermolecular interactions.

2 Results and discussion

2.1. Syntheses and general characterization

The $\text{PPh}_4[\text{Fe}^{\text{III}}(\text{Tp})(\text{CN})_3]\cdot\text{H}_2\text{O}$ complex was prepared in three steps by following our previously reported procedure [30]. First we isolated a $[\text{Fe}^{\text{II}}(\text{Tp})_2]$ complex by direct reaction of the scorpionate ligand, KTp, and a Fe(II) salt. In a second step, the reaction of three equivalents of KCN with the recrystallized dried $[\text{Fe}^{\text{II}}(\text{Tp})_2]$ allows the formation of the tricyanido complex $[\text{Fe}^{\text{II}}(\text{Tp})(\text{CN})_3]^{2-}$. This one is then carefully oxidized by hydrogen peroxide and recrystallized from acetonitrile solution after a salt metathesis reaction. The ammonium salt of the $[\text{Fe}^{\text{III}}(\text{Tp}^*)(\text{CN})_3]^-$ building block can be obtained similarly in three steps, as reported by Holmes *et coll.* [31], however the result is more uncertain. The instability of the first intermediate product, $[\text{Fe}^{\text{II}}(\text{Tp}^*)_2]$, (that need to be immediately used), the potential hazards related to the partial solvent removal from a hydrogen peroxide contaminated acetonitrile solution, and its layering by diethyl ether are major drawbacks. We thus developed a new one-step synthesis whose yield is lower (*ca.* 32%) but which allows a straightforward access to single crystals of $\text{PPh}_4[\text{Fe}^{\text{III}}(\text{Tp}^*)(\text{CN})_3]\cdot\text{CH}_3\text{CN}$ (crystallographic data and a view of the crystal structure, Fig. S1, are given in supplementary material). In this synthesis, the degassed solution containing equivalent amount of Fe(II) salt and KTp* is to be added to the cyanide solution shortly after its preparation as $[\text{Fe}^{\text{II}}(\text{Tp}^*)_2]$ tends to precipitate over time. Then the oxidation is carried out by opening the flask to the air. As shown in supplementary material (Fig. S2), the redox potential of the obtained $\text{PPh}_4[\text{Fe}^{\text{III}}(\text{Tp}^*)(\text{CN})_3]\cdot\text{CH}_3\text{CN}$ complex (-1.00 V to be compared with -0.82 V for $[\text{Fe}^{\text{III}}(\text{Tp})(\text{CN})_3]^-$; *versus* $[\text{Fe}^{\text{III/II}}(\text{Cp})_2]$, 10^{-3} M in CH_3CN) allows a clean oxidation by air's oxygen in acetonitrile, avoiding so the critical oxidation step by hydrogen peroxide.

The square complexes were obtained by self-assembling the $[\text{Fe}^{\text{III}}(\text{Tp})(\text{CN})_3]^-$ or $[\text{Fe}^{\text{III}}(\text{Tp}^*)(\text{CN})_3]^-$ building blocks with the *in-situ* formed $[\text{Fe}^{\text{II}}(\text{bik})_2(\text{S})_2]^{2+}$ complexes in alcoholic or acetonitrile solutions. While the use of FeCl_2 salt leads to the crystallization of the previously reported $\{\text{Fe}^{\text{III}}_2\text{Fe}^{\text{II}}_2\}^{2+}$ square complex with the $[\text{Fe}^{\text{III}}(\text{Tp})(\text{CN})_3]^-$ complex acting as counter ion,[22] the presence of fluoroborate or perchlorate anions in the solution (coming from the use of $\text{Fe}^{\text{II}}(\text{BF}_4)_2$ or $\text{Fe}^{\text{II}}(\text{ClO}_4)_2$ salts) leads to the fast crystallization of the dicationic $\{\text{Fe}^{\text{III}}_2\text{Fe}^{\text{II}}_2\}\text{X}_2$ square complexes ($\text{X} = \text{ClO}_4, \text{BF}_4$) in relatively good yield (**2**: 40%; **3**: 60%, **4**: 60%).

The compounds were all characterized by FT-IR spectroscopy. This technique is very useful to characterize the electronic states of cyanido-bridged complexes as the stretching cyanide vibrations are sensitive to the oxidation state of the coordinated metal ions and to the bridging mode of the cyanide (bridging and non bridging). Typically, non bridging $\text{Fe}^{\text{III}}\text{-CN}$ moieties are observed in the range 2130-2110 cm^{-1} , as observed for the precursors: 2123 cm^{-1} for $\text{PPh}_4[\text{Fe}^{\text{III}}(\text{Tp}^*)(\text{CN})_3]\cdot\text{CH}_3\text{CN}$ 2121 cm^{-1} for $\text{PPh}_4[\text{Fe}^{\text{III}}(\text{Tp})(\text{CN})_3]\cdot\text{H}_2\text{O}$. In contrast stretching vibrations due to bridging cyanide

moieties are expected at higher wavenumber (*ca.* > 2145 cm^{-1}). Here the observed cyanide stretching vibrations of **2-4** are reported in the table 1 together with other characteristic FT-IR peaks. They are very similar for all compounds and reveal the presence of one non-bridging Fe^{III} -CN unit and two different Fe^{III} -CN- Fe^{II} bridges in agreement with the crystal structure of the compounds (see below). The elemental analyses carried out on microcrystalline samples agree with the above formula for **4**, while a higher amount of water molecules (5 H_2O) is found in **2** in comparison to the crystal structure (2 H_2O), and a lower amount of CH_3CN is found for **3**, in comparison to the crystal structure. This can be associated to the presence of disordered water molecules in the crystal lattice of **2** and a partial loss of solvent molecule in **3**.

Table 1.

Analytical and selected infra-red data of 2, 3 and 4

compounds	Selected FT-IR vibration (cm^{-1})					Analyses (%) ^a		
	ν_{CN} bridging	ν_{CN} terminal	counter ions	ν_{BH}	$\nu_{\text{C=O}}$	C	H	N
2	2160	2130	1093, 1064, 1054	2538	1634	42.88	4.43	23.49
	2147		(ClO_4^-)			(42.73)	(4.68)	(23.53)
3	2160	2113	1076, 1064, 1045	2503	1632	41.45	3.60	27.39
	2148		(ClO_4^-)			(41.23)	(3.52)	(27.14)
4	2161	2113	1109, 1094, 1045, 995	2510	1633	39.47	3.80	26.78
	2148		(BF_4^-)			(41.27)	(3.80)	(26.40)

^a calculated data are given in parentheses for the formula $\{[\text{Fe}^{\text{III}}(\text{Tp}^*)(\text{CN})_3]_2[\text{Fe}^{\text{II}}(\text{bik})_2]\}_2(\text{ClO}_4)_2 \cdot 5\text{H}_2\text{O}$ (**2**), $\{[\text{Fe}^{\text{III}}(\text{Tp})(\text{CN})_3]_2[\text{Fe}^{\text{II}}(\text{bik})_2]\}_2(\text{ClO}_4)_2 \cdot \text{CH}_3\text{CN}$ (**3**), $\{[\text{Fe}^{\text{III}}(\text{Tp})(\text{CN})_3]_2[\text{Fe}^{\text{II}}(\text{bik})_2]\}_2(\text{BF}_4)_2 \cdot 2\text{CH}_3\text{OH}$ (**4**)

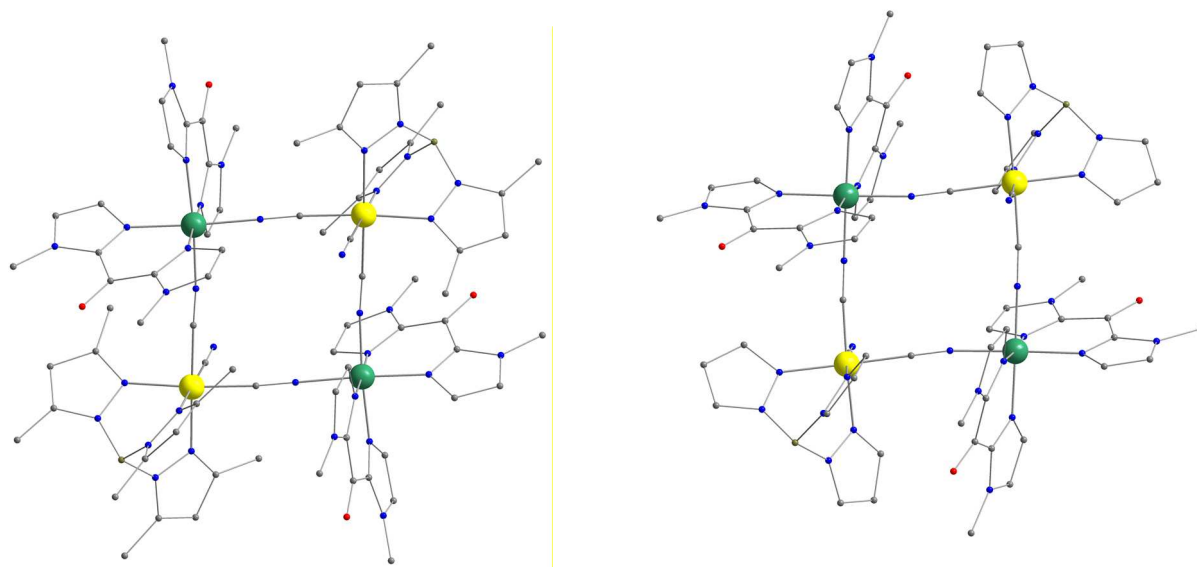


Fig. 1. Perspective views of the $\{\text{Fe}^{\text{III}}_2\text{Fe}^{\text{II}}_2\}$ square complexes **2** (left) and **3** (right). C: grey, N: blue, O: red, B: pink-grey, Fe^{III} : yellow, Fe^{II} : green. Hydrogen atoms are omitted for clarity.

2.2. Description of the structures

Table 2
Crystal data and structure refinement parameters for **2-4**

Compounds	2	3	4
Formula	C ₇₂ H ₈₈ B ₂ Fe ₄ N ₃₄ O ₁₄ Cl ₂	C ₆₄ H ₆₆ B ₂ Fe ₄ N ₃₆ O ₁₂ Cl ₂	C ₆₂ H ₆₈ B ₄ Fe ₄ N ₃₄ O ₆ F ₈
Fw (g/mol)	1969.62	1847.34	1804.04
Crystal system	triclinic	monoclinic	monoclinic
<i>a</i> (Å)	13.430(3)	15.2373(4)	14.9451(5)
<i>b</i> (Å)	13.470(3)	18.5182(4)	18.3777(6)
<i>c</i> (Å)	13.907(3)	15.1215(4)	15.5415(5)
α (°)	102.34(3)	90	90
β (°)	108.67(3)	110.4755(3)	101.927(2)
γ (°)	107.01(3)	90	90
V (Å ³)	2143.9(12)	3997.24(17)	4176.4(2)
Z	1	2	2
Space group	<i>P</i> -1	<i>P</i> 2 ₁ / <i>c</i>	<i>P</i> 2 ₁ / <i>c</i>
μ (cm ⁻¹)	0.808	0.861	0.771
ρ (g cm ⁻³)	1.525	1.535	1.485
Merging R	0.241	0.0925	0.038
<i>R</i> ^a	0.0877	0.0507	0.0601
<i>R</i> _w ^b	0.1582 (0.1819) ^c	0.1196 (0.1324) ^c	0.1789(0.2049) ^c
Gof-fit	0.997	0.963	0.988
Δρ _{min} (e Å ⁻³)	-2.82	-0.574	-1.53
Δρ _{max} (e Å ⁻³)	1.42	0.657	1.88
T (K)	200	140	200

$$^a R = \frac{\sum ||F_o| - |F_c||}{\sum |F_o|}$$

$$^b [\sum w(|F_o| - |F_c|)^2 / \sum w F_o^2]^{1/2}$$

^c For *I* > 2σ (for all data in parentheses)

Red prismatic crystals of **1** and orange-red square-like crystals of **3-4** suitable for single crystal X-ray diffraction experiment were obtained by slow evaporation of the mother solutions. The crystal data were all collected at low temperature (200 or 140 K). Compound **2** and **3-4** crystallize in the *P*-1 and *P*2₁/*c* space groups, respectively. The structures of **2-4** consist of centrosymmetric dicationic cyanide-bridged tetrametallic units {Fe^{III}₂Fe^{II}₂}, perchlorate (**2-3**) or tetrafluoroborate (**4**) counter ions and lattice solvent molecules. The mixed valence tetrametallic units are made of [Fe^{III}(L)(CN)₃]⁻ complex units (L = Tp* for **2** and L = Tp for **1, 3 and 4**) acting as metalloligand (through *cis*-coordinated cyanide) toward divalent Fe(II) ions. The coordination sphere of the Fe(II) ions is completed by two bidentate α-ketone-β-diimine ligands. The tetrametallic core of **2-4** exhibits a [2+2] type diamond-like geometry whose main angles are reported in table 3. The edge distances in **2** are slightly longer than those found in **3-4**, in agreement with the slightly longer Fe^{II}-ligand bond distances. This is likely due to the spin-state of the Fe(II) ions, which is expected to be purely low-spin at 200 K in **3-4** while it may contain some HS component in **2**, as shown by the magnetic measurements (see below). In all complexes, only moderate deviations from linearity are observed on the both side of the cyanide bridges as shown in Table 3.

Both Fe^{II} and Fe^{III} ions exhibit slightly distorted octahedral coordination sphere. The Fe^{II} ions are in a *N*₆ coordination sphere formed by four N atoms of the bik ligands and two N atoms of the cyanide located in *cis* position. The distortion of the coordination sphere can be evaluated by the octahedral distortion, Σ , defined as the sum of the deviation to 90° of the twelve angles around the metal atom. The octahedral distortion, Σ , measured at 200 K amount to 23.2°, 20.8° and 25.0° for **2-4**, respectively. These moderate values agree with the essentially LS states of the complexes **2-4** at 200 K. This is confirmed by the averaged Fe^{II}-N bond lengths (1.981, 1.952, 1.953 Å for 1,2 and 3), which compare well with those found in similar Fe(II) low-spin complexes.[32,22,33]

The Fe^{III} coordination environment is formed by three imine moieties of the pyrazolyl groups and by the carbon atoms of three cyanides. The Fe-C_{CN} bond lengths (average of 1.920, 1.911, 1.912 Å for **2-4**) are in agreement with those previously reported for similar Fe^{III}-LS complexes.[34,31] The Fe^{III}-N_(Tp/Tp*) bond lengths are longer with mean values of 2.007, 1.977 and 1.975 Å for **2-4**. The octahedral distortion, Σ , increases upon coordination of the *N*- donor atom. They amount to 26.8°, 22.4°, 29.9° in **2-4**, respectively, to be compare with 17.9° and 18.5 ° in the PPh₄[Fe^{III}(Tp*)(CN)₃] CH₃CN and PPh₄[Fe^{III}(Tp)(CN)₃] H₂O precursors.[34,31]

Finally, the square units are well separated from each other by the counter ions and the solvent lattice molecules. The shortest metal-metal distances are over 7.5 Å in **3-4** (see table 3). In the case of **2**, a water molecule establishes a hydrogen bridge between the non-bridging cyanide and an oxygen atom of the perchlorate counter ion, a feature commonly observed in these materials.

Table 3
Selected M-M distances,^a bond lengths (Å) and angles (degrees) for **2-4**

Compounds	2	3	4
Fe ^{III} -Fe ^{II} -Fe ^{III}	96.0°	94.5°	91.9°
Fe ^{II} -Fe ^{III} -Fe ^{II}	84.0°	85.4°	88.1°
Fe ^{III} -CN-Fe ^{II}	5.038-5.038	4.954-4.964	4.947-4.971
Fe ^{II} -N _(CN)	1.961(6)-1.976(7)	1.918(3)-1.924(3)	1.918(2)-1.928(2)
Fe ^{II} -N _{bik}	1.973(7)-1.996(6)	1.966(3)-1.986(3)	1.964(2)-1.982(2)
Fe ^{III} -C _(CN) (average)	1.910(9)-1.930(8) (1.920)	1.901(4)-1.930(5) (1.911)	1.897(3)-1.934(3)(1.912)
Fe ^{III} -N _(Tp/Tp*) (average)	1.985(6)-2.024(6) (2.007)	1.963(3)-1.986(3) (1.977)	1.972(2)-1.978(2) (1.975)
Fe ^{II} -NC	174.3 -179.1°	171.4-175.9°	173.3-171.7°
Fe ^{III} -CN	174.4(6)-177.6(7)	174.2-178.2°	177.4-178.4°
Σ Fe ^{II}	23.2°	20.8°	25.0°
Σ Fe ^{III}	26.8°	22.4°	29.9°
Fe...Fe (shortest) ^b	9.46	7.617	7.540

^a all distances are given with an error of 6 to 9 on the last digit | ^b shortest intermolecular Fe-Fe distance

2.3. Magnetic Properties

The magnetic properties of **2-4** are shown in Figure 2 as the $\chi_M T$ products *versus* temperature (χ_M is the molar magnetic susceptibility per $\{\text{Fe}_2^{\text{II}}\text{Fe}^{\text{III}}_2\}$ formula unit). The $\chi_M T$ product of compound **2** shows a sigmoidal curve whose shape is typical of spin-crossover complexes. The $\chi_M T$ variation between low and high temperature, *ca.* $7.1 \text{ cm}^3 \text{ mol}^{-1} \text{ K}$, suggests an almost complete LS \leftrightarrow HS conversion for the two Fe(II) ions, the expected value being $2 \times 3.6 = 7.2 \text{ cm}^3 \text{ mol}^{-1} \text{ K}$, with $S = 2$, $g \approx 2.2$. The transition temperature, $T_{1/2} = 227 \text{ K}$, is lower than those measured in our previous studies on SCO molecule based on the $\{\text{Fe}(\text{bik})_2(\text{N-})_2\}$ unit. The $\chi_M T$ value measured at low temperature, *ca.* $1.4 \text{ cm}^3 \text{ mol}^{-1} \text{ K}$ at 20 K, is ascribed to the presence of two Fe(III) LS ions ($\chi_M T \approx 0.4 \text{ cm}^3 \text{ mol}^{-1} \text{ K}$ at low temperature for each Fe^{III} ion) and possibly to a small amount of residual Fe(II) HS. Once heated at 400 K in the magnetometer, the spin transition is only slightly shifted toward lower temperature with $T_{1/2} \approx 223 \text{ K}$ (Fig. S3). This shift is likely due to the loss of crystallization solvent. In order to check this hypothesis, an *ex-situ* desolvated sample of **2** was studied. The sample was prepared by heating the crystals in a TGA under a N₂ gas flow up to 80°C. The resulting $\chi_M T$ curve matches well with that obtained for the sample desolvated inside the magnetometer (Fig. S3).

In contrast with **2**, the compounds **3** and **4** do not show a full sigmoidal curve in the 10-400 K temperature range, but only an increase of the $\chi_M T$ products above room temperature that suggests the occurrence of gradual spin-state conversion at high temperatures. The $\chi_M T$ values measured at 400 K, *ca.* 3.2 and $3.7 \text{ cm}^3 \text{ mol}^{-1} \text{ K}$ for **3** and **4**, account for roughly 25% and 32% of high-spin Fe(II) and indicate transition temperatures that are above 400 K. The $\chi_M T$ products measured at low temperature for **3** and **4**, $\chi_M T \approx 1.10 \text{ cm}^3 \text{ mol}^{-1} \text{ K}$ at 20 K, are also coherent with the occurrence of two low-spin Fe^{II} and two low-spin Fe^{III} ions. Here the non-Curie behaviour observed between 20 and 350 K (a slight slope is observed on the $\chi_M T$ vs T curves) is due to the spin-orbit coupling occurring in the $^3\text{T}_{1g}$ ground state term of the low-spin $[\text{Fe}^{\text{III}}(\text{Tp})(\text{CN})_3]^-$ subunit.[35] It is also worth noticing that the spin transition in the compounds **3** and **4** are reversible. Upon cooling from 400 K, the $\chi_M T$ curves superimpose with that of the fresh compounds (see Fig. S4).

The magnetic curve of **2**, which shows a complete and gradual spin-crossover can be simulated using the Slichter-Drickammer mean-field model (equation 1) in order to extract the thermodynamic parameters associated to the spin-state equilibrium and to evaluate the cooperativity.[36]

$$\ln[(1 - n_{HS})/(1 - f_{HS})] = [\Delta H + \Gamma(f_{HS} + 1 - 2n_{HS})]/RT - \Delta S/R \quad (1)$$

In equation 1, ΔH and ΔS are the enthalpy and entropy variations associated to the spin transition, n_{HS} is the HS molar fraction and f_{HS} is the residual HS molar fraction at low temperature. Γ is the

Figure 3, all the irradiations lead to a rapid and efficient increase of the χ_{MT} product of **2** for the six wavelengths that were probed. As for **1**, a plateau is reached after only *ca.* 20 min.[22] The irradiation at 635, 808 and 900 nm are the most efficient ones. These wavelengths correspond to MLCT band of the $[\text{Fe}^{\text{II}}(\text{bik})_2(\text{N-})_2]$ units.[22] The χ_{MT} saturation value obtained in **2**, *ca.* $12 \text{ cm}^3 \text{ mol}^{-1} \text{ K}$, is notably higher than that found in **1**. It is also higher than that obtained at room temperature. This suggests the occurrence of ferromagnetic interactions in the photo-excited state. Actually both ferromagnetic and antiferromagnetic exchange pathways can be expected in a $\{\text{Fe}^{\text{III}}_{\text{LS}}\text{-CN-Fe}^{\text{II}}_{\text{HS}}\}$ bridge. However it has already been observed that the ferromagnetic interaction can dominate in similar low-dimensional systems.[40,41] The drop of the χ_{MT} product at low temperature (below 10 K) is likely due to the occurrence of antiferromagnetic intermolecular interaction or/and magnetic anisotropy effects. The stability of the metastable state of **2** was then probed by measuring the χ_{MT} versus T curve after irradiation (at 808 nm or 900nm), from 2 to 100 K (Figure 4). Upon heating the magnetization relaxes back to the diamagnetic state and becomes close to initial value at *ca.* 35 K. This behaviour is similar to that observed for **1**. Overall, the LIESST effect is much more efficient in **2** than in **3** and **4**. This is coherent with previous studies, which reported that the higher the thermal transition is (the higher the energy difference between the LS ground state and the HS state is), the smaller the stabilization of the metastable state is, and the lower the relaxation temperature is.[42–44]

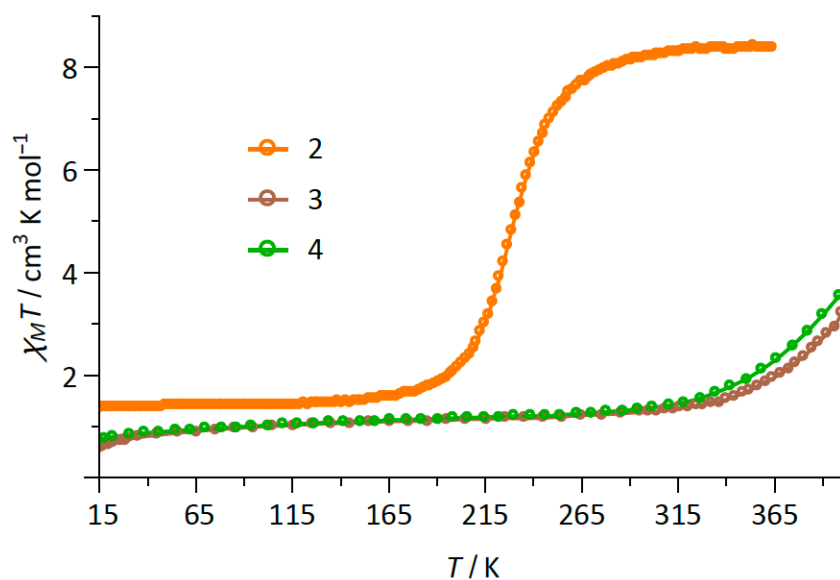


Fig. 2. Magnetic properties of **2-4** depicted as the χ_{MT} versus T curve.

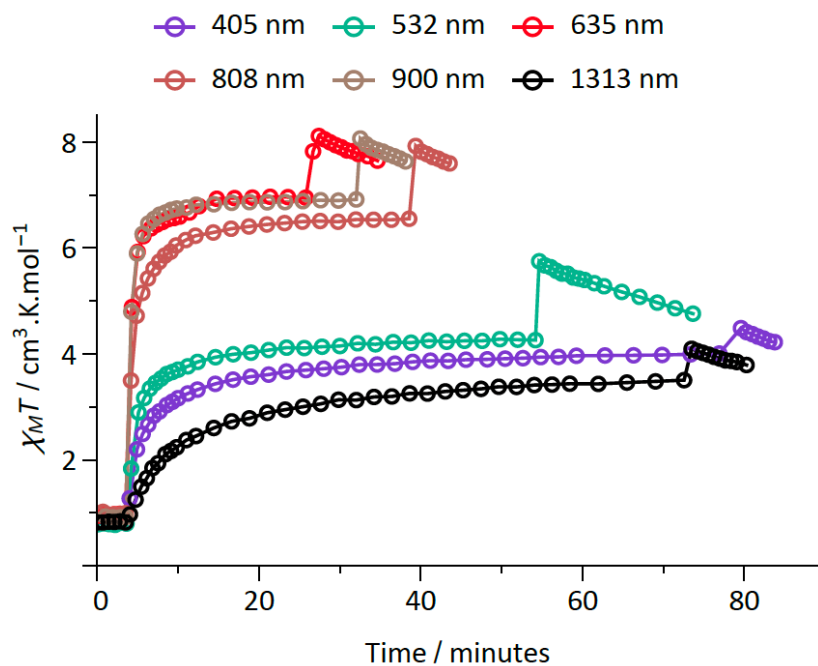


Fig. 3. Measurement of the $\chi_M T$ product *versus* time under laser light irradiation (ca. 5 mW/cm²) at 20 K for the compound **2**. The first jump corresponds to the moment the light is switched on (photomagnetic effect) while the second jump corresponds to the moment the light is switched off and the temperature of the sample decreases.

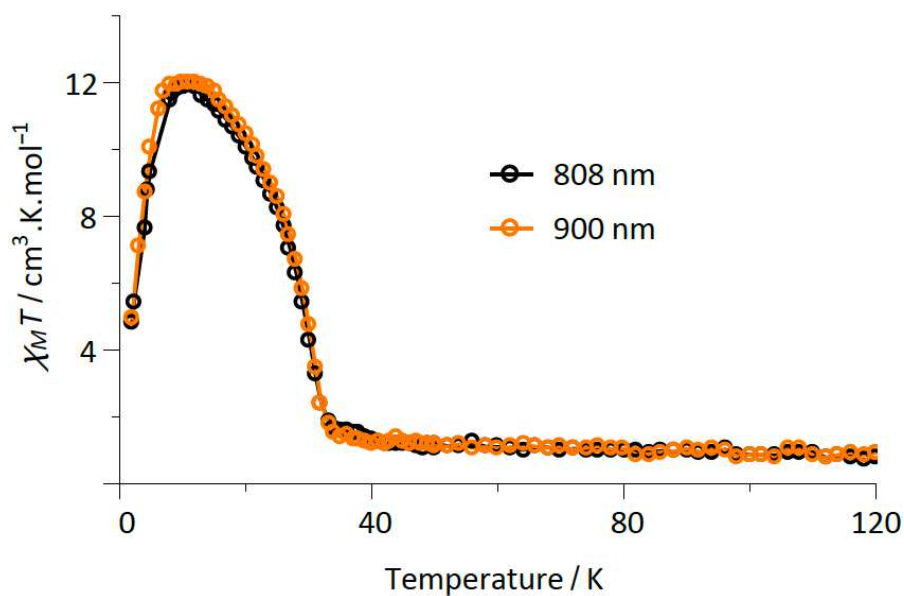


Fig. 4. Measurement of the $\chi_M T$ product after laser light irradiation at 20 K ($H = 1T$). The sample is measured from 2 to 100 K at 0.4 K/min.

3 Conclusions

Continuing our investigation on the $[\text{Fe}^{\text{II}}(\text{bik})_2(\text{N}^-)_2]$ SCO units, we reported here three novel mixed valence cyanide-bridged $\{\text{Fe}^{\text{III}}_2\text{Fe}^{\text{II}}_2\}\text{X}_2$ square complexes ($\text{X} = \text{ClO}_4, \text{BF}_4$) which are reminiscent of our previously published $\{[\text{Fe}^{\text{III}}(\text{Tp})(\text{CN})_3]_2[\text{Fe}^{\text{II}}(\text{bik})_2]_2\} \cdot [\text{Fe}^{\text{III}}(\text{Tp})(\text{CN})_3]_2$ square complex. These squares were obtained by reacting $[\text{Fe}^{\text{II}}(\text{bik})_2(\text{S})_2]^{2+}$ with the $[\text{Fe}^{\text{III}}(\text{Tp})(\text{CN})_3]^-$ or $[\text{Fe}^{\text{III}}(\text{Tp}^*)(\text{CN})_3]^-$ N-donor metalloligands. The compounds **3** and **4** based on the $[\text{Fe}^{\text{III}}(\text{Tp})(\text{CN})_3]^-$ metalloligand exhibit spin-crossover at high temperature ($T_{1/2} > 400$ K) and no (**3**) or moderate (**4**) photomagnetic effect. In contrast, the use of the $[\text{Fe}^{\text{III}}(\text{Tp}^*)(\text{CN})_3]^-$ as N-donor metalloligand leads to a shift of the spin-crossover of the $[\text{Fe}^{\text{II}}(\text{bik})_2(\text{N}^-)_2]$ units toward lower temperature, with $T_{1/2} = 233$ K. The spin-state change in **2** is gradual and the thermodynamic parameter extracted from the magnetic measurements leads to weak value of cooperative factor ($\Gamma < \square\square\square\square_{1/2}$) in agreement with the absence of significant intermolecular interactions in **2**. The decrease of the $T_{1/2}$ temperature is associated to a stabilization of the high-spin metastable state and thus a more efficient LIESST effect. Remarkably, the irradiation with different laser lights covering the visible and NIR range leads to significant photomagnetic effect. However, the strongest increase of magnetization is observed when irradiating the sample at 635, 808 or 900 nm, in the region corresponding to LMCT band of the $[\text{Fe}^{\text{II}}(\text{bik})_2(\text{N}^-)_2]$ units. The resulting photoinduced $\chi_{\text{M}}T$ values are high and indicate the occurrence of ferromagnetic interactions in the $\{\text{Fe}^{\text{III}}_{\text{LS}}\text{-CN-Fe}^{\text{II}}_{\text{HS}}\}$ metastable state.

Finally, this experimental study nicely complete our previous investigations on the photomagnetic properties of the $[\text{Fe}^{\text{II}}(\text{bik})_2(\text{N}^-)_2]$ SCO units. When confronting all these studies, it appears that the nature of the N-donor metalloligand strongly influences the energy of the most efficient laser light inducing the LIESST effect. While the most efficient irradiation is located at 405 nm when using the $[\text{Mo}(\text{CN})_8]^{3-}$ as N-donor ligands, it becomes 635 nm for the bik N-donor ligand, 750 nm for the $[\text{Fe}^{\text{III}}(\text{Tp})(\text{CN})_3]^-$ metalloligand, and 900 nm for the NCS^- N-donor ligand. The present study leads to the best results as a remarkable magnetization increase is observed with the same efficiency at 635, 808 and 900 nm when using the $[\text{Fe}(\text{Tp}^*)(\text{CN})_3]^-$ N-donor metalloligand. The correlation with the absorption spectra of these compounds do not lead to clear conclusion as all of them are dominated by a intense LMCT bands of the $[\text{Fe}^{\text{II}}(\text{bik})_2(\text{N}^-)_2]$ units. We believe that the rationalization of this behaviour would require advanced physical measurements to better investigate the excitation states involved in the LIESST effect.

4 Experimental Section

4.1. General

All chemicals used were of reagent grade quality. They were purchased from commercial sources and used as received. The bik ligand was prepared as reported Braussaud *et al.*[45]. The

$\text{PPh}_4[\text{Fe}^{\text{III}}(\text{Tp})(\text{CN})_3]\cdot\text{H}_2\text{O}$ complex was prepared in three steps by following our previously reported procedure [30].

4.2. Preparations

4.2.1. $\text{PPh}_4[\text{Fe}^{\text{III}}(\text{Tp}^*)(\text{CN})_3] \text{CH}_3\text{CN}$

A degassed solution of KTp^* (319 mg, 1.0 mmol) in 5 mL methanol was added dropwise to a methanolic solution of $\text{FeCl}_2\cdot 4\text{H}_2\text{O}$ (199 mg, 1.0 mmol in 15 mL). The violet suspension was stirred for one hour, then added dropwise to a methanolic solution of KCN (214 mg, 3.3 mmol). The resulting red suspension was stirred at room temperature overnight and the methanol was evacuated to dryness. The red resulting solid was redissolved in acetonitrile and filtered. Crystals of $\text{K}[\text{Fe}^{\text{III}}(\text{Tp}^*)(\text{CN})_3]$ were produced by slow evaporation of the acetonitrile solution. Crystals of $\text{PPh}_4[\text{Fe}^{\text{III}}(\text{Tp}^*)(\text{CN})_3] \text{H}_2\text{O}$ suitable for X-ray diffraction analysis were produced in 1-2 weeks by slow evaporation of an acetonitrile solution of $\text{K}[\text{Fe}^{\text{III}}(\text{Tp}^*)(\text{CN})_3]$ in which was added one equivalent of tetraphenylphosphonium chloride and a small amount of water. Yield: 32%. Elemental analysis (%): calculated for $\text{C}_{42}\text{H}_{42}\text{BFeN}_9\text{P} \cdot \text{CH}_3\text{CN} \cdot 0.5\text{H}_2\text{O}$: C 64.41, H 5.65, N 17.07; found: C 64.71, H 5.43, N 16.79. ESI-MS m/z (%): 431.14 (100) $[\text{Fe}^{\text{III}}(\text{Tp}^*)(\text{CN})_3]^-$, 339.13 (100), $[\text{PPh}_4]^+$.

4.2.2. $\{[\text{Fe}^{\text{III}}(\text{Tp}^*)(\text{CN})_3]_2[\text{Fe}^{\text{II}}(\text{bik})_2]\}_2(\text{ClO}_4)_2 \cdot 2\text{H}_2\text{O}$ (2)

0.05 mmol of $\text{Fe}^{\text{II}}(\text{ClO}_4)_2\cdot 6\text{H}_2\text{O}$ (19 mg,) and bik ligand (19 mg, 0.1 mmol) were dissolved in 15 mL of a methanol/water (5/1) mixture. The resulting deep dark blue solution was added to a solution of $\text{K}[\text{Fe}(\text{Tp}^*)(\text{CN})_3]$ (25 mg) in 15 mL of the same mixture of solvents. The purple solution was further stirred about 10 minutes before being filtered. Slow evaporation of the reaction mixture produced carmine red crystals suitable for X-ray diffraction analysis. Yield 40 %.

4.2.3. $\{[\text{Fe}^{\text{III}}(\text{Tp})(\text{CN})_3]_2[\text{Fe}^{\text{II}}(\text{bik})_2]_2\}(\text{ClO}_4)_2 \cdot 2\text{CH}_3\text{CN}$ (3)

0.01 mmol (70.6 mg) of $\text{PPh}_4[\text{Fe}^{\text{III}}(\text{Tp})(\text{CN})_3]\cdot\text{H}_2\text{O}$ was dissolved in ca. 10 mL of acetonitrile and added dropwise to a solution containing $[\text{Fe}(\text{bik})_2(\text{S})_2](\text{ClO}_4)_2$ (S = solvent). The air stable $[\text{Fe}^{\text{II}}(\text{bik})_2(\text{S})_2]\text{Cl}_2$ complex was prepared *in situ* by reacting approximately 0.01 mmol (36.2 mg) of $\text{Fe}(\text{ClO}_4)_2\cdot 6\text{H}_2\text{O}$ and 0.02 mmol (38 mg) of the bik ligand in ca. 5 mL of acetonitrile. The resulting bluish-red solution was stirred at room temperature for 30 min and then filtered. Slow evaporation of the filtrate under ambient conditions afforded orange-red plate-like crystal of $\{[\text{Fe}^{\text{III}}(\text{Tp})(\text{CN})_3]_2[\text{Fe}^{\text{II}}(\text{bik})_2]_2\}(\text{ClO}_4)_2 \cdot 2\text{CH}_3\text{CN}$ (3). Yield 60 %.

4.2.4. $\{[\text{Fe}^{\text{III}}(\text{Tp})(\text{CN})_3]_2[\text{Fe}^{\text{II}}(\text{bik})_2]\}_2(\text{BF}_4)_2 \cdot 2\text{CH}_3\text{OH}$ (4)

0.01 mmol (70.6 mg) of $\text{PPh}_4[\text{Fe}^{\text{III}}(\text{Tp})(\text{CN})_3]\cdot\text{H}_2\text{O}$ was dissolved in ca. 10 mL of a methanolic/acetonitrile mixture and added dropwise to a solution containing $[\text{Fe}(\text{bik})_2(\text{S})_2]\text{Cl}_2$. The air stable $[\text{Fe}(\text{bik})_2(\text{S})_2]\text{Cl}_2$ complex was prepared *in situ* by reacting of 0.01 mmol (33.8 mg) of

Fe(BF₄)₂·6H₂O and 0.02 mmol (38 mg) of the bik ligand in *ca.* 5 mL of methanol. The resulting bluish-red solution was stirred at room temperature for 30 min and then filtered. Slow evaporation of the filtrate under ambient conditions afforded orange-red plate-like crystal of {[Fe^{III}(Tp)(CN)₃]₂[Fe^{II}(bik)₂]₂(BF₄)₂·2CH₃OH (**4**). Yield 60 %.

4.3. X-ray data collection and refinement

A single crystal of each compound was selected, mounted onto a cryoloop, and transferred in a cold nitrogen gas stream. Intensity data were collected with graphite-monochromated Mo-K α radiation ($\lambda = 0.71073 \text{ \AA}$) either with a BRUKER Kappa-APEXII or a RIGAKU-OXFORD Sapphire 3 Xcalibur diffractometer. Data collection, unit-cell parameters refinement, integration and data reduction were performed with CrysAlis (Oxford) or APEX2 (Bruker) softwares. Multi-scan absorption corrections were applied. The structure were solved with either ShelxS86,[46] Superflip[47] or Sir97[48] programs and refined by full-matrix least-squares methods using SHELXL-14[49] or CRYSTALS[50].

4.4. Physical techniques

Elemental analyses (C, H, N, Co, Mn, and Ni) were performed by the Service Central d'Analyse du CNRS (France). IR spectra were recorded on a Perkin–Elmer 882 spectrophotometer as KBr pellets. Variable-temperature (2.0–400 K) magnetic susceptibility measurements in the direct-current (dc) mode were carried out with a Quantum Design SQUID magnetometer using applied magnetic fields of 0.5 T ($T > 30 \text{ K}$) and 0.025 T ($T < 30 \text{ K}$). The magnetic data were corrected for the diamagnetism of the constituent atoms and the sample holder. The samples of **2-4** were measured as crystalline powders, removed from their mother solution directly before the measurements and introduced into the magnetometer at 200 K to avoid the loss of solvent crystallization molecules.

5 Supplementary material

X-ray crystallographic files in CIF format (excluding structure factors) for **2-4** and **5** are available from the Cambridge Crystallographic Data Centre, 12 Union road, Cambridge CB2 1EZ, UK (fax: +44-1223-336033; email: deposit@ccdc.cam.ac.uk or www: <http://www.ccdc.cam.ac.uk>) on request, on quoting the deposition number CCDC 1891890 (**2**), 1891892 (**3**), 1891891 (**4**) and 1891893 (**5**).

Acknowledgement

Financial support was received from the Ministère Français de l'enseignement et de la recherche et du Centre National de la Recherche Scientifique (CNRS), the DFG-funded transregional collaborative research centre SFB/TRR 88 "Cooperative effects in homo- and heterometallic complexes (3MET)" (projectB4).

References

- [1] M. Irie, Photochromism: Memories and Switches Introduction, *Chemical Reviews*. 100 (2000) 1683–1684. doi:10.1021/cr980068l.
- [2] B.L. Feringa, ed., *Molecular switches*, Wiley-VCH-Verl, Weinheim, 2011.
- [3] M.A. Halcrow, ed., *Spin-crossover materials: properties and applications*, Wiley, Chichester, 2013.
- [4] J.E. Green, J. Wook Choi, A. Boukai, Y. Bunimovich, E. Johnston-Halperin, E. Delonno, Y. Luo, B.A. Sheriff, K. Xu, Y. Shik Shin, H.-R. Tseng, J.F. Stoddart, J.R. Heath, A 160-kilobit molecular electronic memory patterned at 1011 bits per square centimetre, *Nature*. 445 (2007) 414–417. doi:10.1038/nature05462.
- [5] H.J. Shepherd, I.A. Gural'skiy, C.M. Quintero, S. Tricard, L. Salmon, G. Molnár, A. Bousseksou, Molecular actuators driven by cooperative spin-state switching, *Nature Communications*. 4 (2013). doi:10.1038/ncomms3607.
- [6] R. Vincent, S. Klyatskaya, M. Ruben, W. Wernsdorfer, F. Balestro, Electronic read-out of a single nuclear spin using a molecular spin transistor, *Nature*. 488 (2012) 357–360. doi:10.1038/nature11341.
- [7] G. Molnár, S. Rat, L. Salmon, W. Nicolazzi, A. Bousseksou, Spin Crossover Nanomaterials: From Fundamental Concepts to Devices, *Advanced Materials*. 30 (2018) 1703862. doi:10.1002/adma.201703862.
- [8] A. Dei, Photomagnetic Effects in Polycyanometallate Compounds: An Intriguing Future Chemically Based Technology?, *Angewandte Chemie International Edition*. 44 (2005) 1160–1163. doi:10.1002/anie.200461413.
- [9] M.C. Muñoz, J.A. Real, Thermo-, piezo-, photo- and chemo-switchable spin crossover iron(II)-metallocyanate based coordination polymers, *Coordination Chemistry Reviews*. 255 (2011) 2068–2093. doi:10.1016/j.ccr.2011.02.004.
- [10] Y.-S. Meng, O. Sato, T. Liu, Manipulating Metal-to-Metal Charge Transfer for Materials with Switchable Functionality, *Angewandte Chemie International Edition*. 57 (2018) 12216–12226. doi:10.1002/anie.201804557.
- [11] O. Sato, Y. Einaga, T. Iyoda, A. Fujishima, K. Hashimoto, Reversible photoinduced magnetization, *Journal of the Electrochemical Society*. 144 (1997) L11–L13.
- [12] O. Sato, Y. Einaga, A. Fujishima, K. Hashimoto, Photoinduced Long-Range Magnetic Ordering of a Cobalt–Iron Cyanide, *Inorganic Chemistry*. 38 (1999) 4405–4412. doi:10.1021/ic980741p.
- [13] G. Champion, V. Escax, C. Cartier dit Moulin, A. Bleuzen, F. Villain, F. Baudelet, E. Dartyge, M. Verdagner, Photoinduced Ferrimagnetic Systems in Prussian Blue Analogues $C^I_x Co_4 [Fe(CN)_6]_y$ ($C^I =$ Alkali Cation). 4. Characterization of the Ferrimagnetism of the Photoinduced Metastable State in $Rb_{1.8} Co_4 [Fe(CN)_6]_{3.3} \cdot 13H_2O$ by K Edges X-ray Magnetic Circular Dichroism, *Journal of the American Chemical Society*. 123 (2001) 12544–12546. doi:10.1021/ja011297j.
- [14] C. Mathonière, Metal-to-Metal Electron Transfer: A Powerful Tool for the Design of Switchable Coordination Compounds: Metal-to-Metal Electron Transfer: A Powerful Tool for the Design of Switchable Coordination Compounds, *European Journal of Inorganic Chemistry*. 2018 (2018) 248–258. doi:10.1002/ejic.201701194.
- [15] D. Aguilà, Y. Prado, E.S. Koumoussi, C. Mathonière, R. Clérac, Switchable Fe/Co Prussian blue networks and molecular analogues, *Chemical Society Reviews*. 45 (2016) 203–224. doi:10.1039/C5CS00321K.

- [16] A. Mondal, Y. Li, M. Seuleiman, M. Julve, L. Toupet, M. Buron-Le Cointe, R. Lescouëzec, On/Off Photoswitching in a Cyanide-Bridged $\{Fe_2Co_2\}$ Magnetic Molecular Square, *Journal of the American Chemical Society*. 135 (2013) 1653–1656. doi:10.1021/ja3087467.
- [17] M. Nihei, Y. Sekine, N. Suganami, K. Nakazawa, A. Nakao, H. Nakao, Y. Murakami, H. Oshio, Controlled Intramolecular Electron Transfers in Cyanide-Bridged Molecular Squares by Chemical Modifications and External Stimuli, *Journal of the American Chemical Society*. 133 (2011) 3592–3600. doi:10.1021/ja109721w.
- [18] Y.-Z. Zhang, P. Ferko, D. Siretanu, R. Ababei, N.P. Rath, M.J. Shaw, R. Clérac, C. Mathonière, S.M. Holmes, Thermochromic and Photoresponsive Cyanometalate Fe/Co Squares: Toward Control of the Electron Transfer Temperature, *Journal of the American Chemical Society*. 136 (2014) 16854–16864. doi:10.1021/ja508280n.
- [19] M. Urdampilleta, C. Ayela, P.-H. Ducrot, D. Rosario-Amorin, A. Mondal, M. Rouzières, P. Dechambenoit, C. Mathonière, F. Mathieu, I. Dufour, R. Clérac, Molecule-based microelectromechanical sensors, *Scientific Reports*. 8 (2018). doi:10.1038/s41598-018-26076-2.
- [20] S. De, J.-R. Jiménez, Y. Li, L.-M. Chamoreau, A. Flambard, Y. Journaux, A. Bousseksou, R. Lescouëzec, One synthesis: two redox states. Temperature-oriented crystallization of a charge transfer $\{Fe_2Co_2\}$ square complex in a $\{FeIILS Co IIILS\}$ diamagnetic or $\{Fe IIILS Co IIHS\}$ paramagnetic state, *RSC Advances*. 6 (2016) 17456–17459.
- [21] J. Mercuriol, Y. Li, E. Pardo, O. Risset, M. Seuleiman, H. Rousselière, R. Lescouëzec, M. Julve, $[FeIILSCoIIILS]_2 \rightleftharpoons [FeIIILSCoIIHS]_2$ photoinduced conversion in a cyanide-bridged heterobimetallic molecular square, *Chemical Communications*. 46 (2010) 8995. doi:10.1039/c0cc02024a.
- [22] A. Mondal, Y. Li, P. Herson, M. Seuleiman, M.-L. Boillot, E. Rivière, M. Julve, L. Rechinat, A. Bousseksou, R. Lescouëzec, Photomagnetic effect in a cyanide-bridged mixed-valence $\{FeII_2FeIII_2\}$ molecular square, *Chemical Communications*. 48 (2012) 5653. doi:10.1039/c2cc17835d.
- [23] A. Mondal, Y. Li, L.-M. Chamoreau, M. Seuleiman, L. Rechinat, A. Bousseksou, M.-L. Boillot, R. Lescouëzec, Photo- and thermo-induced spin crossover in a cyanide-bridged $\{Mo^V_2Fe^{II}_2\}$ rhombus molecule, *Chem. Commun.* 50 (2014) 2893–2895. doi:10.1039/C3CC49164A.
- [24] S. De, L.-M. Chamoreau, H. El Said, Y. Li, A. Flambard, M.-L. Boillot, S. Tewary, G. Rajaraman, R. Lescouëzec, Thermally-Induced Spin Crossover and LIESST Effect in the Neutral $[FeI(Mebik)_2(NCX)_2]$ Complexes: Variable-Temperature Structural, Magnetic, and Optical Studies (X = S, Se; Mebig = bis(1-methylimidazol-2-yl)ketone), *Frontiers in Chemistry*. 6 (2018). doi:10.3389/fchem.2018.00326.
- [25] S. De, S. Tewary, D. Garnier, Y. Li, G. Gontard, L. Lisnard, A. Flambard, F. Breher, M.-L. Boillot, G. Rajaraman, R. Lescouëzec, Solution and Solid-State Study of the Spin-Crossover $[Fe^{II}(R-bik)_3](BF_4)_2$ Complexes (R = Me, Et, Vinyl): Solution and Solid-State Study of the Spin-Crossover $[Fe^{II}(R-bik)_3](BF_4)_2$ Complexes (R = Me, Et, Vinyl), *European Journal of Inorganic Chemistry*. 2018 (2018) 414–428. doi:10.1002/ejic.201701013.
- [26] G. Lemercier, N. Bréfuel, S. Shova, J.A. Wolny, F. Dahan, M. Verelst, H. Paulsen, A.X. Trautwein, J.-P. Tuchagues, A Range of Spin-Crossover Temperature $T_{1/2} > 300$ K Results from Out-of-Sphere Anion Exchange in a Series of Ferrous Materials Based on the 4-(4-Imidazolylmethyl)-2-(2-imidazolylmethyl)imidazole (trim) Ligand, $[Fe(trim)_2]X_2$ (X = F, Cl, Br, I): Comparison of Experimental Results with Those Derived from Density Functional Theory Calculations, *Chemistry - A European Journal*. 12 (2006) 7421–7432. doi:10.1002/chem.200501249.
- [27] S. Vela, H. Paulsen, Deciphering crystal packing effects in the spin crossover of six $[Fe^{II}(2-pic)_3]Cl_2$ solvatomorphs, *Dalton Transactions*. (2019). doi:10.1039/C8DT04394A.
- [28] M. Buron-Le Cointe, J. Hébert, C. Baldé, N. Moisan, L. Toupet, P. Guionneau, J.F. Létard, E. Freysz, H. Cailleau, E. Collet, Intermolecular control of thermoswitching and photoswitching phenomena in two

spin-crossover polymorphs, *Physical Review B*. 85 (2012). doi:10.1103/PhysRevB.85.064114.

[29] C. Bartual-Murgui, S. Vela, M. Darawsheh, R. Diego, S.J. Teat, O. Roubeau, G. Aromí, A probe of steric ligand substituent effects on the spin crossover of Fe(II) complexes, *Inorganic Chemistry Frontiers*. 4 (2017) 1374–1383. doi:10.1039/C7QI00347A.

[30] R. Lescouëzec, J. Vaissermann, F. Lloret, M. Julve, M. Verdaguer, Ferromagnetic Coupling between Low- and High-Spin Iron(III) Ions in the Tetranuclear Complex $f ac - \{ [Fe^{III} \{ HB(pz)_3 \} (CN)_2 (\mu-CN)]_3 Fe^{III} (H_2O)_3 \} \cdot 6H_2O$ ($[HB(pz)_3]^-$ = Hydrotris(1-pyrazolyl)borate), *Inorganic Chemistry*. 41 (2002) 5943–5945. doi:10.1021/ic020374o.

[31] D. Li, S. Parkin, G. Wang, G.T. Yee, S.M. Holmes, Synthesis and Spectroscopic and Magnetic Characterization of Tris(3,5-dimethylpyrazol-1-yl)borate Iron Tricyanide Building Blocks, a Cluster, and a One-Dimensional Chain of Squares, *Inorganic Chemistry*. 45 (2006) 1951–1959. doi:10.1021/ic051044h.

[32] M. Nihei, M. Ui, H. Oshio, Cyanide-bridged tri- and tetra-nuclear spin crossover complexes, *Polyhedron*. 28 (2009) 1718–1721. doi:10.1016/j.poly.2008.10.051.

[33] P. Gütllich, Y. Garcia, H.A. Goodwin, Spin crossover phenomena in Fe(II) complexes, *Chemical Society Reviews*. 29 (2000) 419–427. doi:10.1039/b003504I.

[34] R. Lescouëzec, J. Vaissermann, L.M. Toma, R. Carrasco, F. Lloret, M. Julve, *mer*- $[Fe^{III} (bpca)(CN)_3]^-$: A New Low-Spin Iron(III) Complex to Build Heterometallic Ladder-like Chains, *Inorganic Chemistry*. 43 (2004) 2234–2236. doi:10.1021/ic030284z.

[35] K. Ridier, A. Mondal, C. Boilleau, O. Cador, B. Gillon, G. Chaboussant, B. Le Guennic, K. Costuas, R. Lescouëzec, Polarized Neutron Diffraction to Probe Local Magnetic Anisotropy of a Low-Spin Fe(III) Complex, *Angewandte Chemie International Edition*. 55 (2016) 3963–3967. doi:10.1002/anie.201511354.

[36] C.P. Slichter, H.G. Drickamer, Pressure-Induced Electronic Changes in Compounds of Iron, *The Journal of Chemical Physics*. 56 (1972) 2142–2160. doi:10.1063/1.1677511.

[37] S.E. Creutz, J.C. Peters, Spin-State Tuning at Pseudo-tetrahedral d^6 Ions: Spin Crossover in $[BP_3]Fe^{II}-X$ Complexes, *Inorganic Chemistry*. 55 (2016) 3894–3906. doi:10.1021/acs.inorgchem.6b00066.

[38] H. Petzold, P. Djomgoue, G. Hörner, J.M. Speck, T. Rüffer, D. Schaarschmidt, 1H NMR spectroscopic elucidation in solution of the kinetics and thermodynamics of spin crossover for an exceptionally robust Fe²⁺ complex, *Dalton Transactions*. 45 (2016) 13798–13809. doi:10.1039/C6DT01895E.

[39] V. Martínez, A.B. Gaspar, M.C. Muñoz, G.V. Bukin, G. Levchenko, J.A. Real, Synthesis and Characterisation of a New Series of Bistable Iron(II) Spin-Crossover 2D Metal-Organic Frameworks, *Chemistry - A European Journal*. 15 (2009) 10960–10971. doi:10.1002/chem.200901391.

[40] J.-L. Wang, H.-L. Zhu, L. Zhao, L.-X. Ren, C.-Y. Duan, T. Liu, Controllable antiferromagnetic to ferromagnetic coupling in polynuclear Fe(III)–Co(II) heterobimetallic complexes, *Inorganic Chemistry Communications*. 76 (2017) 55–58. doi:10.1016/j.inoche.2017.01.013.

[41] H. Zheng, L. Zhao, T. Liu, P.-F. Zhuang, C.-Q. Jiao, J.-X. Hu, Y. Xu, C. He, C.-Y. Duan, Two cyanobridged $\{Fe^{III}4M^{II}2\}_c$ (M=Fe, Co) hexanuclear complexes with dominant ferromagnetic interactions, *Inorganic Chemistry Communications*. 57 (2015) 33–35. doi:10.1016/j.inoche.2015.04.015.

[42] J.-F. Létard, J.S. Costa, S. Marcen, C. Carbonera, C. Desplanches, A. Kobayashi, N. Daro, P. Guionneau, J.-P. Ader, Does cooperativity influence the lifetime of the photo-induced HS state?, *Journal of Physics: Conference Series*. 21 (2005) 23–29. doi:10.1088/1742-6596/21/1/004.

[43] J.-F. Létard, P. Guionneau, O. Nguyen, J.S. Costa, S. Marcén, G. Chastanet, M. Marchivie, L. Goux-Capes, A Guideline to the Design of Molecular-Based Materials with Long-Lived Photomagnetic Lifetimes, *Chemistry - A European Journal*. 11 (2005) 4582–4589. doi:10.1002/chem.200500112.

- [44] A. Hauser, C. Enachescu, M.L. Daku, A. Vargas, N. Amstutz, Low-temperature lifetimes of metastable high-spin states in spin-crossover and in low-spin iron(II) compounds: The rule and exceptions to the rule, *Coordination Chemistry Reviews*. 250 (2006) 1642–1652. doi:10.1016/j.ccr.2005.12.006.
- [45] N. Braussaud, T. Rüther, K.J. Cavell, B.W. Skelton, A.H. White, Bridged 1-Methylbisimidazoles as Building Blocks for Mixed Donor Bi- and Tridentate Chelating Ligands, *Synthesis*. 2001 (2001) 0626–0632. doi:10.1055/s-2001-12351.
- [46] G.M. Sheldrick, A short history of *SHELX*, *Acta Crystallographica Section A Foundations of Crystallography*. 64 (2008) 112–122. doi:10.1107/S0108767307043930.
- [47] L. Palatinus, G. Chapuis, *SUPERFLIP* – a computer program for the solution of crystal structures by charge flipping in arbitrary dimensions, *Journal of Applied Crystallography*. 40 (2007) 786–790. doi:10.1107/S0021889807029238.
- [48] A. Altomare, M.C. Burla, M. Camalli, G.L. Cascarano, C. Giacovazzo, A. Guagliardi, A.G.G. Moliterni, G. Polidori, R. Spagna, *SIR 97*: a new tool for crystal structure determination and refinement, *Journal of Applied Crystallography*. 32 (1999) 115–119. doi:10.1107/S0021889898007717.
- [49] G.M. Sheldrick, Crystal structure refinement with *SHELXL*, *Acta Crystallographica Section C Structural Chemistry*. 71 (2015) 3–8. doi:10.1107/S2053229614024218.
- [50] D.J. Watkin, C.K. Prout, J.R. Carruthers, P.W. Betteridge, R.I. Cooper, *CRYSTALS issue 11*, Chemical Crystallography Laboratory, Oxford, 2003.